

Video Self-Distillation for Single-Image Encoders: A Step Toward Physically Plausible Perception

Marcel Simon¹ Tae-Ho Kim¹ Seul-Ki Yeom¹

Abstract

Self-supervised image encoders such as DINO (Caron et al., 2021) have recently gained significant interest for learning robust visual features without labels. However, most SSL methods train on static images and miss the temporal cues inherent in videos. We introduce a video-distilled *single-image* encoder trained to predict the next-frame representation from the current frame. This simple objective injects 3D spatial and temporal priors without optical flow or tracking. When pre-training on a single 2-hour video, our approach raises the mean Intersection-over-Union (mIoU) on ADE20K from 35.0 (DoRA (Venkataramanan et al., 2024)) to 36.4 while remaining a drop-in replacement for image-only pipelines. Our results highlight video self-distillation as a lightweight route to geometry-aware perception—an essential ingredient for physically plausible world models and *Physical AI*.

1. Introduction and Related Work

Self-supervised learning (SSL) has reached parity with full supervision for image encoders, powered by self-distillation (Grill et al., 2020; Caron et al., 2021; Oquab et al., 2023), contrastive objectives (Chen et al., 2020; He et al., 2020), and masked reconstruction (He et al., 2022). Yet these *static-image* paradigms overlook the temporal coherence and multi-view geometry that videos offer for free. Consecutive frames provide virtually unlimited dense supervision and better match downstream settings such as robotic control in *Physical AI*.

Early video-SSL work produced purely video backbones—e.g. TimeSformer (Bertasius et al., 2021) and MaskFeat (Wei et al., 2022). More recently, distilling *single-image* encoders from videos has drawn attention.

¹Nota AI GmbH, Friedrichstrasse 200, 10117 Berlin, Germany. Correspondence to: Seul-Ki Yeom <skyeom@nota.ai>.

DoRA (Venkataramanan et al., 2024) tracks objects to create masked images used as additional data for self-distillation, but still optimizes each frame independently, limiting temporal reasoning. PooDLe (Wang et al., 2024) enforces equivariance under optical-flow warps, but flow estimation is slow, brittle, and fails under occlusion.

Our approach. We address these issues with a training-time change: a lightweight predictor head regresses the teacher representation of frame $t+\Delta$ from the student encoding of frame t . The head is discarded afterward, so inference remains fast while the static-image backbone gains 3D and temporal priors. When pre-training on a single 2-hour video, our approach surpasses previous work in semantic segmentation with less training time and a simpler architecture.

3D-aware features are especially valuable for embodied agents. Current Vision–Language–Action (VLA) systems such as GR00T N1 (Brohan et al., 2025) and OpenVLA (Kim et al., 2024) rely on encoders trained on static images; our dense, temporally informed representations supply complementary cues that might unlock more reliable physical reasoning.

Contributions.

- **Next-frame objective:** We introduce a next-frame objective that injects temporal priors into an off-the-shelf static-image encoder
- **Dense prediction head:** We design a lightweight dense-prediction head only used at training time.

2. Proposed Method

Problem setup. Given an unlabeled video $V = \{x_1, \dots, x_T\}$ we form clips $\mathcal{C}_t = \{x_{t+i\Delta}\}_{i=0}^{K-1}$, where Δ is a stride hyper-parameter (default $\Delta=30$ frames) and $K=3$. We apply a pre-crop and then mostly follow (Caron et al., 2021) for each frame, but apply the same pre-crop and global crop to all frames to allow dense prediction. Local views are obtained for each frame starting with $x_{t+\Delta}$.

Architecture. Our architecture follows the self-distillation framework presented in (Caron et al., 2021). Both teacher and student share a ViT-S backbone as well as the projection

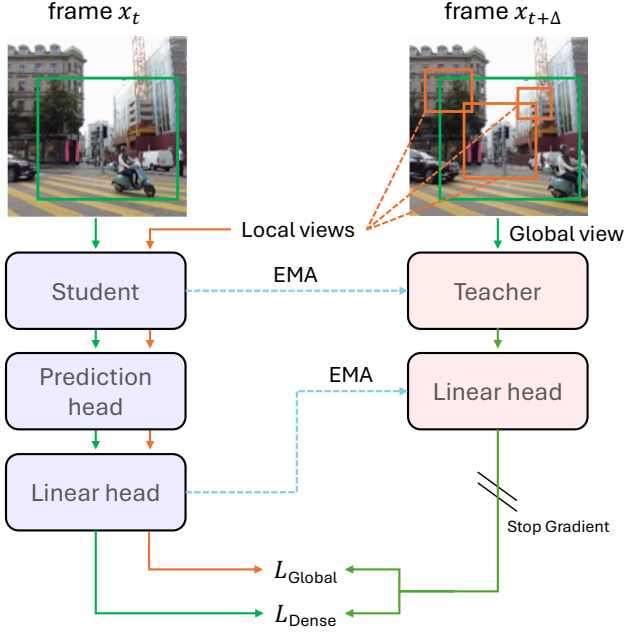


Figure 1. Overview of dense prediction during training. The student encodes a frame and a dense prediction head is used to estimate the features of the teacher for the next frame. Exponential moving average (EMA) is used to update the teacher.

head. In contrast to DINO, we add an additional 2-layer MLP as well as two attention blocks between the student backbone and projection head. The attention blocks provide predicting capabilities, while the MLP separates the shared image encoder from these prediction blocks. This prediction head is only used during training and also exclusive to the student. Teacher weights are an exponential moving average of the student, identical to DINO, and no gradients flow through the teacher.

Loss functions. During training, the student processes all global views except the last one as well as all local views. The teacher processes only the global views starting with $x_{t+2\Delta}$. We then optimize two complementary terms.

(i) Dense next-frame loss.

Let P be the number of patch tokens. For every consecutive pair $(x_j, x_{j+\Delta})$ with $j \in \{t, \dots, t + (K-2)\Delta\}$, the teacher T produces patch tokens $z_{j+\Delta}^T \in \mathbb{R}^{P \times d}$ while the student S predicts $\hat{z}_{j \rightarrow j+\Delta}^S$ from x_j . We compute the averaged cross-entropy for each such pair and each patch

$$\mathcal{L}_{\text{dense}} = \frac{1}{K-1} \sum_{j=t}^{t+(K-2)\Delta} \text{P-CE}(\sigma_{\tau_{\text{T}}}(z_{j+\Delta}^{\text{T}}), \sigma_{\tau_{\text{S}}}(\hat{z}_{j \rightarrow j+\Delta}^{\text{S}})), \quad (1)$$

where P-CE denotes the averaged per-patch cross-entropy to make notation easier to read.

(ii) **Global loss.** Each future frame x_j with $j \in \{t +$

$\Delta, \dots, t + (K - 1)\Delta\}$ has L local crops. Denote its teacher [CLS] token output by \tilde{z}_j^T and the ℓ -th student prediction by $\tilde{z}_{j,\ell}^S$ for $\ell = 1, \dots, L$. The loss

$$\mathcal{L}_{\text{global}} = \frac{1}{(K-1)L} \sum_{j=t+\Delta}^{t+(K-1)\Delta} \sum_{\ell=1}^L \text{CE}(\sigma_{\tau_{\text{T}}}(\tilde{z}_j^{\text{T}}), \sigma_{\tau_{\text{S}}}(\tilde{z}_{j,\ell}^{\text{S}})). \quad (2)$$

encourages feature consistency across different augmentations of the same image.

Total objective. The final training loss is the unweighted average $\mathcal{L} = 0.5 \mathcal{L}_{\text{dense}} + 0.5 \mathcal{L}_{\text{global}}$. While the loss computation is similar to DINO, the features used are different. The global loss is computed using only the *[CLS] tokens* of views of the same frame. In contrast, the dense loss is computed using the *patch tokens* of consecutive frames.

Why prediction rather than reconstruction? Regressing teacher features teaches the student to preserve only those signals that remain stable over a temporal offset Δ , implicitly suppressing fleeting noise (e.g., specular flicker) and promoting geometrically consistent embeddings. The resulting encoder is a drop-in replacement for single-image pipelines—unlike multi-frame backbones—and is therefore directly usable in VLA-based architectures for robotics and other time-critical settings that demand real-time, physically plausible observations.

3. Experiments

We evaluate the quality of our approach by evaluating the trained static-image encoder on dense prediction tasks.

3.1. Experimental Setup

Data and sampling. All models are trained from scratch on the publicly available *Walking Tours Venice* 60 fps video (1920×1080) (Venkataramanan et al., 2024). Clips of $K=3$ consecutive frames $\{x_t, x_{t+\Delta}, x_{t+2\Delta}\}$ are drawn with stride $\Delta=30$ unless stated otherwise.

Augmentations. Each frame receives a pre-crop with target area 0.05–0.20 to approximate ImageNet statistics, followed by DINO multi-crop (Caron et al., 2021). The same *global* 224² crop is applied to all three frames, but the color augmentations are independent. We sample five 96² *local* crops from $x_{t+\Delta}$ and $x_{t+2\Delta}$ each.

Training. We train a ViT-S/16 backbone on four NVIDIA RTX 4090 GPUs with an aggregate batch size of 256. Running 100 epochs on the *WT Venice* video finishes in roughly one day. All frames are pre-extracted as JPEGs to bypass runtime decoding. The remaining hyperparameters and schedules match those of (Caron et al., 2021).

Evaluation. Semantic segmentation is measured on

Table 1. Semantic segmentation on ADE20K (mIoU) when pre-trained on WT Venice for 100 epochs. [†] result from (Wang et al., 2024). DoRA results are computed using the official checkpoint.

Method	Backbone	UperNet	Fast-LP
PooDLe	ResNet-50	36.6 [†]	14.6 [†]
DINO (frames)	ViT-S/16	31.7	12.9
+ pre-crop		35.1	15.8
+ time-aug $\Delta=5$		34.9	15.9
DoRA	ViT-S/16	35.0	17.0
Ours (dense+global loss)	ViT-S/16	36.4	18.3
<i>global-loss only</i>		34.5	15.6
<i>dense-loss only</i>		36.2	17.4

Table 2. Object detection on MS-COCO. Training uses a 512×512 crop for efficiency reasons.

Method	COCO-2017 mAP
DINO on frames + pre-crop	33.3
+ time-aug $\Delta=5$	33.3
DoRA	33.0
Ours ($\Delta=30$)	33.5

ADE20K (Zhou et al., 2017) with full UperNet fine-tuning and a *fast linear* probe (Fast-LP) with frozen backbone, 1000 iterations, and batch size 64 for ablations. Object detection uses MS COCO-2017 (Lin et al., 2014). The iBOT evaluation protocol and code (Zhou et al., 2022) is used to provide comparable results to (Venkataramanan et al., 2024). Teacher weights are used at test time. We retrain all baselines ourselves, but use the official DoRA checkpoint for 100 epochs on WT Venice due to excessive training time when using the official codebase.

3.2. Main Results

Semantic segmentation We present the results for semantic segmentation in Table 1. Our approach improves over DoRA by +1.4 mIoU on UperNet and by +1.1 mIoU on the fast linear probe. We also compare to several DINO baselines. When using plain DINO and treating the frames of the video as independent images, the accuracy drops by up to 5.2 reaching only 12.9 mIoU on the linear probe. Pre-cropping proves to be fundamental and improves this baseline by almost 3 points. This indicates that the video frames of WT Venice contain too many different objects when using a single global objective. The last two rows present the mIoU when using only one of the two loss terms and the combined loss achieves the best result.

We also provide a time-augmentation baseline for comparison. In this case, we use regular DINO but global and local views are split among two consecutive frames instead of using the same frame for all views. Smaller strides give better results for this baseline, so we use only $\Delta = 5$. As can be seen, the time-based augmentation alone does not

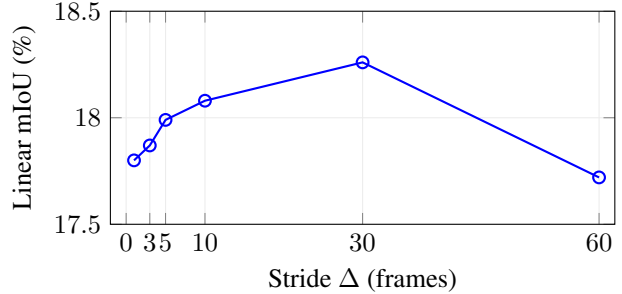


Figure 2. Effect of prediction stride Δ on ADE20K fast-linear accuracy. Performance peaks at $\Delta \approx 30$ and plateaus for longer horizons.

give the same benefit as our approach.

Finally, we also include the results from (Wang et al., 2024), a recent publication that uses optical flow to compute a dense and global loss across consecutive frames. Our approach does not require any optical flow and still achieves comparable results.

Object detection Table 2 shows results for object detection on MS COCO. Our approach slightly improves the results of DoRA by 0.5 mAP while the training time of our approach is significantly faster.

3.3. Stride Ablation

Fig. 2 presents results for different values of Δ . Longer strides modestly improve segmentation up to $\Delta = 30$, after which gains saturate, confirming that our approach benefits from extended temporal context, but even works in a frame-by-frame regime.

4. Conclusion

We propose a lightweight next-frame distillation framework that injects temporal and geometric priors into an off-the-shelf image encoder while preserving single-frame inference speed. Our approach outperforms the tracking-based DoRA on ADE20K and COCO, illustrating that video self-distillation can serve as a pragmatic building block for the *physically plausible world models* sought by Physical AI models. Our approach does not require any labels and hence can be directly applied and trained on application specific tasks where sample video data is available.

5. Acknowledgments

This work was supported by the Technology Innovation Program (RS-2024-00468747, Development of AI and Lightweight Technology for Embedding Multisensory Intelligence Modules) funded by the Ministry of Trade Industry & Energy (MOTIE, Korea).

References

- Bertasius, G., Wang, H., and Torresani, L. Is space-time attention all you need for video understanding? In *Int. Conf. Mach. Learn.*, 2021.
- Brohan, A. et al. GR00T N1: An open foundation model for generalist humanoid robots. *arXiv preprint arXiv:2503.14734*, 2025.
- Caron, M., Touvron, H., Misra, I., Jégou, H., Mairal, J., Bojanowski, P., and Joulin, A. Emerging properties in self-supervised vision transformers. In *Int. Conf. Comput. Vis.*, 2021.
- Chen, T., Kornblith, S., Norouzi, M., and Hinton, G. A simple framework for contrastive learning of visual representations. In *Int. Conf. Mach. Learn.*, pp. 1597–1607, 2020.
- Grill, J.-B., Strub, F., Altch’e, F., Tallec, C., Richemond, P., Buchatskaya, E., Doersch, C., Pires, B., Guo, Z. D., Azar, M., Piot, B., Guez, A., Pietquin, O., Kavukcuoglu, K., Larochelle, H., Lanctot, M., and Schmitt, S. Bootstrap your own latent: A new approach to self-supervised learning. In *Adv. Neural Inform. Process. Syst.*, 2020.
- He, K., Fan, H., Wu, Y., Xie, S., and Girshick, R. Momentum contrast for unsupervised visual representation learning. In *IEEE Conf. Comput. Vis. Pattern Recog.*, pp. 9729–9738, 2020.
- He, K., Chen, X., Xie, S., Li, Y., Doll’ar, P., and Girshick, R. Masked autoencoders are scalable vision learners. In *IEEE Conf. Comput. Vis. Pattern Recog.*, 2022.
- Kim, M. J., Pertsch, K., Karamcheti, S., et al. Openvla: An open-source vision–language–action model. *arXiv preprint arXiv:2406.09246*, 2024.
- Lin, T.-Y., Maire, M., Belongie, S., and et al. Microsoft coco: Common objects in context. *Eur. Conf. Comput. Vis.*, 2014. URL <https://cocodataset.org/>.
- Oquab, M., Darcet, T., Moutakanni, T., Vo, H. V., Szafraniec, M., Khalidov, V., Fernandez, P., Haziza, D., Massa, F., El-Nouby, A., Assran, M., Ballas, N., Galuba, W., Howes, R., Huang, P., Li, S., Misra, I., Rabbat, M., Sharma, V., Synnaeve, G., Xu, H., Jégou, H., Mairal, J., Labatut, P., Joulin, A., and Bojanowski, P. DINOv2: Learning robust visual features without supervision. *arXiv preprint arXiv:2304.07193*, 2023.
- Venkataramanan, S., Rizve, M. N., Carreira, J., Asano, Y. M., and Avrithis, Y. Is imagenet worth 1 video? learning strong image encoders from 1 long unlabelled video. In *Int. Conf. Learn. Represent.*, 2024.
- Wang, A. N., Hoang, C., Xiong, Y., LeCun, Y., and Ren, M. Poodle: Pooled and dense self-supervised learning from naturalistic videos. *Int. Conf. Learn. Represent.*, 2024. URL <https://arxiv.org/abs/2408.11208>.
- Wei, C., Fan, H., Xie, S., Schmid, C., and Doll’ar, P. Masked feature prediction for self-supervised visual pre-training. In *IEEE Conf. Comput. Vis. Pattern Recog.*, 2022.
- Zhou, B., Zhao, H., Puig, X., and et al. Scene parsing through ade20k dataset. *IEEE Conf. Comput. Vis. Pattern Recog.*, 2017. URL <https://ade20k.csail.mit.edu/>.
- Zhou, K., Yang, J., and Loy, C. C. ibot: Image bert pre-training with online tokenizer. In *Int. Conf. Learn. Represent.*, 2022.